Molecular Ecology (2003) **12**, 169–184

Dispersal barriers and isolation among deep-sea mussel populations (Mytilidae: *Bathymodiolus*) from eastern Pacific hydrothermal vents

Y. WON,*† C. R. YOUNG,*‡ R. A. LUTZ§ and R. C. VRIJENHOEK*
**Monterey Bay Aquarium Research Institute, 7700 Sandholdt Road, Moss Landing, CA 95039-0628, USA, †Graduate Program in Ecology & Evolution, Rutgers University, New Brunswick, NJ, USA, ‡Graduate Program in Ecology & Evolutionary Biology, University of California, Santa Cruz, USA, §Institute of Marine and Coastal Sciences, Rutgers University, New Brunswick, NJ, USA*

Abstract

Deep-sea hydrothermal vent species are widely dispersed among habitat islands found along the global mid-ocean ridge system. We examine factors that affect population structure, gene flow and isolation in vent-endemic mussels of the genus *Bathymodiolus* from the eastern Pacific Ocean. Mussels were sampled from localities including the Galapagos Rift (GAR, 0°48′ N; 86°10′ W) and the East Pacific Rise (EPR, 13° N to 32° S latitude) across a maximum distance of 4900 km. The sampled range crossed a series of topographical features that interrupt linear aspects of the ridge system, and it encompassed regions of strong cross-axis currents that could impede along-axis dispersal of mussel larvae. Examinations of mitochondrial DNA sequences and allozyme variation revealed significant barriers to gene flow along the ridge axis. All populations from the GAR and EPR from 13° N to 11° S were homogeneous genetically and appeared to experience unimpeded high levels of interpopulational gene flow. In contrast, mussels from north and south of the Easter Microplate were highly divergent (4.4%), possibly comprising sister-species that diverged after formation of the microplate ≈ 4.5 Ma. Strong cross-axis currents associated with inflated bathymetry of the microplate region may reinforce isolation across this region.

Keywords: allozymes, East Pacific Rise, gene flow, mitochondrial DNA, speciation

Received 20 June 2002; revision received 14 October 2002; accepted 14 October 2002

Introduction

Deep-sea hydrothermal vent communities provide significant exceptions to the spatially continuous and environmentally uniform conditions of the marine abyssal zone (Gage & Tyler 1991; Van Dover 2000). Vents are scattered along the global mid-ocean ridge system, back-arc spreading centres and off-axis submarine volcanoes. These fragmented habitats support dense communities of specialized animals, entirely dependant on chemoautotrophic microbes that exploit energy-rich compounds (H_2S and CH_4) in the vent fluids (Fisher *et al*. 1994; Van Dover & Fry 1994). Characterized as patchy and ephemeral (Grassle 1985; Van Dover & Hessler 1990; Tunnicliffe *et al*. 1998; Desbruyères *et al*. 2000a), discrete vent fields may be separated by a few kilometres along a ridge segment or by hundreds to thousands of kilometres spanning multiple ridge segments. Temporal fluctuations in venting activity and abrupt changes in the geochemical milieu may affect local populations by creating divergent selective regimes and gaps in organismic distributions along a ridge axis (e.g. Jollivet *et al*. 1999; Desbruyères *et al*. 2000a; O'Mullan *et al*. 2001). Topographical features of the mid-ocean ridge system, such as transform faults, ridge offsets, bathymetric inflation and intersecting microplates, can alter oceanic circulation patterns and limit along-axis dispersal (Van Dover *et al*. 2002). The embryos and larvae of some vent animals (e.g. alvinellid polychaetes, Zal *et al*. 1995) are negatively buoyant and may be transported in near-bottom currents along the ridge axis (Kim & Mullineaux 1998). In contrast, buoyant larvae of other species may be entrained in hydrothermal plumes and transported hundreds of metres upward into the water column, above the walls of the ridge axis (Mullineaux *et al*. 1995). Except for one vestimentiferan tubeworm and one alvinellid

Correspondence: R. C. Vrijenhoek. Fax: +831-775-1620; E-mail: vrijen@mbari.org

polychaete, however, little is known about the longevity and transport of embryos or larvae of vent endemic organisms in the water column (Marsh *et al*. 2001; Pradillon *et al*. 2001).

The goal of this study was to identify potential barriers to dispersal of *Bathymodiolus* mussels associated with eastern Pacific hydrothermal vents. This mussel produces large numbers of small eggs that develop into free-swimming planktotrophic larvae, presumed to be capable of long-range dispersal (Lutz *et al*. 1980). A previous genetic study of *B. thermophilus* (Craddock *et al*. 1995), based on eight allozyme loci and mitochondrial restriction fragment length polymorphisms (RFLPs), revealed high rates gene flow among discrete populations along the Galapagos Rift (GAR, 0° N latitude, Fig. 1a) and the northern East Pacific Rise (EPR, 9–13° N). These mussels exhibited no evidence for significant barriers to dispersal or isolation-by-distance across this region. For this study, we examined *Bathymodiolus* mussels from a greatly expanded geographical scale. New samples collected from the southern East Pacific Rise (SEPR), between 7 and 32° S latitude, provided opportunities to consider a variety of geographical and hydrological factors that might impede dispersal. The expanded scale (≈ 4900 km) of the study region undoubtedly exceeds the average dispersal distance of *Bathymodiolus* larvae; thus it is more likely than the previous study to reveal evidence for isolation-by-distance. Between 5 and 14° S latitude (Fig. 1a), the SEPR axis is interrupted by a series of closely

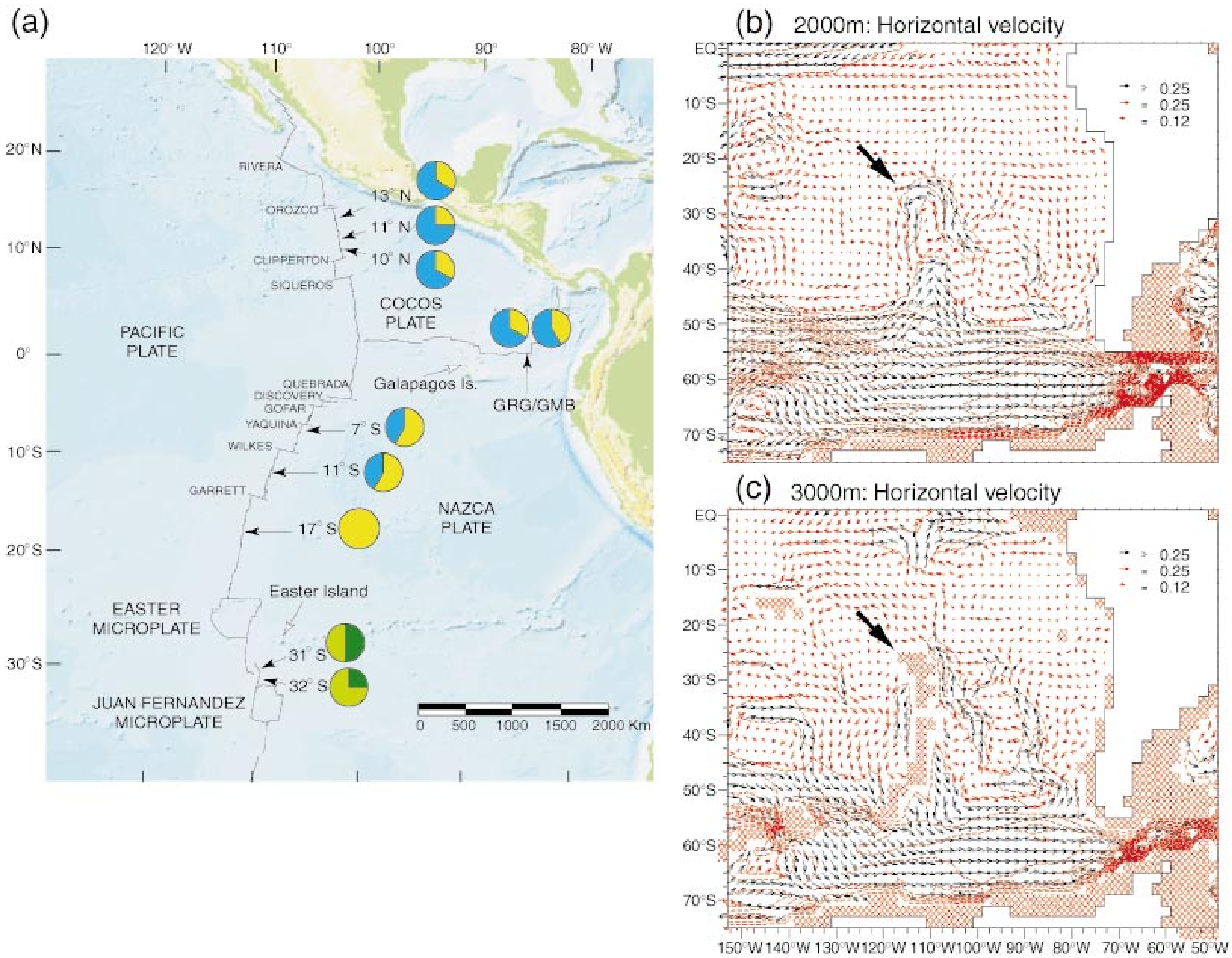

Fig. 1 (a) Map of the south-east Pacific and *Bathymodiolus* sampling locations along the East Pacific Rise (EPR) and Galapagos Rift (GAR). Pie diagrams represent frequencies of mitochondrial COI halpotypes in each sample. Haplotypes colours correspond to branches in neighbour-joining tree (Fig. 2): yellow = Bt1–Bt16 of branch I-A; blue = Bt17–Bt27 of branch I-B, dark green = Bt28–Bt33 of branch II-C, and light green = Bt34–Bt41 of branch II-D. (b) Deep-ocean circulation at 2000 m depth. (c) Circulation at 3000 m depth. The 2000 m velocity vector was modified from published data (Fujio & Imasato 1991), and the 3000 m figure was provided by Dr Shinzou Fujio. Large black arrows indicate the position of the Easter Microplate. Three different arrows shown in upper right represent the strength of each current vector. The velocity of current is cm/s. The crosshatched area is shallower than the depth in question.

stacked ridge offsets (e.g. the Quebrada, Wilkes, Garrett Fracture Zones) that might interrupt along-axis dispersal. The region between 17 and 23° S latitude is known to be among the fastest spreading regions (≈ 18 cm/year) of the global ridge system (Sinton *et al*. 1994). Habitat disruption due to frequent volcanic events may render this portion of the axis inhospitable for mussels, late-successional members of these dynamic communities (see, e.g. Shank *et al*. 1998). The Easter Microplate intersects the SEPR axis between 23 and 27° S, creating a bathymetrically inflated feature that might interrupt connections with mussel populations to the south. Finally, the SEPR axis is intersected by deep-ocean currents (2000–3000 m) in several regions (Lupton & Craig 1981; Fujio & Imasato 1991). Cross-axis currents could displace larvae that are transported in buoyant hydrothermal plumes and disrupt along-axis dispersal. Acting together, oceanic currents and topographic discontinuities in the Southern Hemisphere could create numerous barriers to dispersal of highly vagile mussel larvae.

We examined variation of mitochondrial DNA (mtDNA) and allozyme markers to elucidate population subdivision and to estimate rates of gene flow in *Bathymodiolus* mussels from their known range along the East Pacific Rise and Galapagos Rift. We used a new statistical approach developed by Nielsen & Wakeley (2001) to distinguish limited gene flow from historical isolation in the pattern of the mitochondrial variation. Both historical and incomplete barriers to gene flow revealed by these markers were assessed with respect to deep-ocean circulation patterns and geological features. Our findings are used to erect hypotheses about dispersal barriers that can be tested with parallel phylogeographical studies of codistributed vent-endemic species.

Materials and methods

Specimens

We used the deep ocean submersible *Alvin* to collect *Bathymodiolus* mussels from eight hydrothermal vent fields along the EPR and two vent fields on the GAR (Fig. 1a, Table 1). Specimens were placed in an insulated box containing 2 °C ambient seawater. On board the support vessel, we immediately froze small mussels (up to 25 mm length) at –70 °C. Large mussels were dissected and adductor muscle, gill and mantle tissues were frozen separately at –70 °C. All frozen samples were transported to the land-based laboratory on dry ice and subsequently stored at –80 °C.

mtDNA methods

The CTAB protocol (Doyle & Dickson 1987) was used to isolate whole cellular DNA from tissue digested in 0.05–0.1 g hexadecyl–trimethyl–ammonium bromide. We purified DNA by phenol extraction and ethanol precipitation (Sambrook *et al.* 1989) and rehydrated in 1× TE buffer (10 mM Tris–HCl, pH 7.5; 1 mM EDTA) to a final concentration of 100–500 ng/μl for polymerase chain reaction (PCR) amplification.

Approximately 700 bp of mitochondrial COI were amplified, using universal primers LCO1490 and HCO2198 (Folmer *et al.* 1994), which had a tailing sequence comprised of M13 forward and M13 reverse at the 5′-end of each primer for sequencing with dye-labelled universal primers (LiCor Inc.). The 50 μl amplification reaction mixtures contained 30–100 ng of template DNA, 5 μl 10×

Table 1 *Bathymodiolus* samples examined in this study

Vent locality	Abbr.	Latitude	Longitude	Depth (m)	Dive No.	Date
Galapagos Rift	GAR					
Mussel Bed	GMB	0°47.9′ N	86°09.2′ W	2486	2223	28.V.1990
Rose Garden	GRG	0°48.3′ N	86°13.5′ W	2460	2224	29.V.1990
East Pacific Rise	EPR					
13° N	13N	12°48.7′ N	103°56.7′ W	2636	2228	6.VI.1990
		12°48.6′ N	103°56.5′ W	2630	2229	7.VI.1990
11° N	11N	11°24.9′ N	103°47.3′ W	2515	2226	4.VI.1990
9° N	9N	9°30.9′ N	104°14.5′ W	2585	2350	31.III.1991
		9°33.5′ N	104°15.1′ W	2567	2352	2.IV.1991
		9°50.5′ N	104°17.5′ W	2525	2498	6.III.1992
7° S	7S	7°25.0′ S	107°48.6′ W	2747	3320	23.XII.1998
		7°25.0′ S	107°47.7′ W	2746	3321	24.XII.1998
11° S	11S	11°18.2′ S	110°31.8′ W	2669	3323	27.XII.1998
17° S	17S	17°24.9′ S	113°12.2′ W	2578	3327	31.XII.1998
		17°25.4′ S	113°12.3′ W	2581	3328	1.I.1999
31° S	31S	31°09.3′ S	111°55.9′ W	2333	3337	13.I.1999
		31°09.4′ S	111°55.9′ W	2332	3339	15.I.1999
32° S	32S	31°51.8′ S	112°02.8′ W	2331	3340	16.I.1999

buffer (supplied by manufacturer), 5 µl $MgCl_2$ (2.5 µm), 2 µl of each primer (10 µm final conc.), 2.5 units of *Taq* DNA polymerase (Promega), 5 µl of a 2 mm stock solution of dNTPs, and sterile H_2O to final volume. Amplifications were carried out using 35 cycles at 94 °C/1 min, 50 °C/1 min and 72 °C/1 min, followed by a final extension at 72 °C/7 min.

PCR products were purified by gel excision and cleaned with Qiaquick gel purification kit™, according to the manufacturer's instructions (Qiagen Inc.). Sequencing reactions were performed bi-directionally with dye-labelled M13 forward and reverse primers (LiCor Inc.). Automated sequencing was performed with a LiCor 4200 sequencer (LiCor Inc.) using SequiTherm EXCEL II sequencing protocols (Epicentre Inc.). The resulting COI sequences were aligned using Sequencher (Gene Codes Corporation Inc.), and polymorphic sites were scored by consensus of both directions for each individual.

Pairwise sequence divergence and evolutionary relationships among operational taxonomic units (OTUs) were estimated using MEGA (Version 1.01, Kumar *et al.* 1994). Pairwise sequence divergence estimates are based on the Kimura-2-parameter model (K2P) (Kimura 1980). To estimate bi-directional mean rates of gene flow between populations, pairwise F_{ST} values were estimated using the SITES program (Version 1.1, Hey & Wakeley 1997). To assess population subdivision, we used the exact test of sample differentiation, based on haplotype frequencies (Raymond & Rousset 1995a), using the ARLEQUIN program (Schneider *et al.* 2000).

Allozyme methods

For each mussel, we homogenized ≈ 0.2 g of adductor muscle tissue in an equal volume of grinding buffer (0.01 m Tris, 2.5 mm EDTA, pH 7.0). The homogenate was centrifuged at 12 000 *g* for 20 min to remove tissue debris. We used cellulose acetate gel electrophoresis (CAGE) to screen specimens for multilocus allozymes that had been examined previously (Craddock *et al*. 1995) and found to be consistently scorable in *B. thermophilus*. Electrophoretic conditions, buffer and stains followed Hebert & Beaton (1989) unless otherwise noted (Table 2). In the case of ambiguous electromorphs, allelic identifications were cross-referenced (side-by-side) on CAGE membranes with previously identified electromorphs. The program GENEPOP (Version 3.3, Raymond & Rousset 1995b) was used for population genetic analyses. We used the exact tests of Rousset & Raymond (1995) to assess deviations from random mating expectations. Genic differentiation between populations was assessed with an exact test (Goudet *et al*. 1996). We performed a principal components analysis (PCA) on multilocus allozyme data to investigate relationships among populations. The computer package PCAGEN (Goudet 1999) was used to estimate the percent inertia of each PCA axis and its *P*-value by 1000 randomizations of genotypes.

Tests of isolation vs. gene flow

To test the null hypothesis of isolation between pairs of populations, we used the recently developed likelihood ratio method of Nielsen & Wakeley (2001). The method uses a Markov chain Monte Carlo approach to estimate the posterior distributions of the three parameters of interest (the probability of the parameter values given the data: $f(\Theta \mid X)$, where $\Theta = \{\theta, M, T\}$, $\theta = 4N_e\mu$, $M = 2N_em$ and T = time since divergence of the two populations). In this study, we used the three-parameter model. This model assumes equal sizes of the ancestral population (subscript A) and the two extant populations (subscripts 1 and 2), and it assumes equal migration between the two extant populations (i.e. $\theta = \theta_1 = \theta_2 = \theta_A$ and $M = M_1 = M_2$). The method also estimates T. This method has been extended to

Table 2 Enzymes assayed and buffers used for allozyme analyses

Enzyme	Locus	EC No.	Optimal buffers*
Aspartate aminotransferase	*Aat-2*	2.6.1.2	TC 7.0
Glucose-6-phosphate isomerase	*Gpi*	5.3.1.9	TC 7.0
Isocitrate dehydrogenase	*Idh-2*	1.1.1.42	CA 6.2
Leucine aminopeptidase	*Lap*	3.4.11.1	TC 7.0
Mannose-6-phosphate isomerase	*Mpi*	5.3.1.8	TC 7.0
D-Octopine dehydrogenase	*Opdh*	1.5.1.1	TG 8.5
Peptidase	*Pep-lgg, Pep-ll*	3.4.11 or 3.4.13	TG 8.5
6-Phosphogluconate dehydrogenase	*Pgdh-1*	1.1.1.44	TC 7.0

*The chemical compositions of each buffer to make up one liter volume are as follows: TC 7.0: Trizma base (90.8 g), citric monohydrate (52.5 g), pH = 7.0, and dilution factor for working buffer with deionized water (20×); TG 8.5: Trizma base (30 g), glycine (144 g), pH = 8.5, and dilution factor (10×); CA 6.2: Citric acid monohydrate (42 g), *N*-(3-aminopropyl)-morpholine (50 mL), pH = 6.2, and dilution factor (20×).

a six-parameter model allowing for unequal θ and M, but the six-parameter algorithm was not available from the authors at the time of this study (Nielsen, pers. commun.).

To ensure that the posterior distributions are proper probability distributions, it is necessary to constrain the parameter space over which the search is performed (Nielsen & Wakeley 2001). In practice, this amounts to choosing values for M_{max} and T_{max} as search parameters. We attempted to expand M_{max} and T_{max} to include the maximum estimates of the two parameters. However, for some population comparisons, we were unable to find a maximum below $M_{max} = 100$. In these cases, the likelihood surface is quite flat above $M = 20$, and further increases in M_{max} do little to resolve the estimate. We therefore report the maximum likelihood estimate (MLE) as > 100.

If a uniform prior distribution for the parameter values is assumed (all values of the parameter are equally likely given no information from the data), then the likelihood function, $L(\theta \mid X)$, is given by the posterior distribution (Nielsen & Wakeley 2001). Therefore, it is possible to use a log-likelihood ratio (LR) test to perform a hypothesis test between two nested models. In our case, we are interested in discriminating the hypotheses that the two populations are isolated ($M = 0$) or are exchanging migrants at some rate ($M > 0$). The isolation model (null hypothesis) is considered a nested case of the more general migration model (alternative hypothesis) because the migration parameter is fixed at 0 and is not free to vary. This test is carried out by comparing the log-likelihood ratio of the nested models, $-2(\ln L_{M=0} - \ln L_{max})$, to a χ^2 distribution with 1 degree of freedom.

The migration model allows M to vary between 0 and M_{max}. However, in the isolation model, M is fixed at the boundary of the parameter space ($M = 0$) of the alternative model. In this circumstance, as described in Nielsen & Wakeley (2001), the log-likelihood ratio test statistic should instead be distributed as a random variable that takes the value of 0 with probability 0.5 and takes on a value from a χ^2 distribution with probability 0.5. In practice, one divides the P-value obtained from comparing the LR statistic with a χ^2 distribution by 2 (R. Nielsen, pers. commun.).

Markov chain Monte Carlo methods require a sufficient number of simulated steps of the chain to reach convergence. If too few steps are used in parameter estimation, the estimate will be biased and will depend on the initial parameter values (Nielsen & Wakeley 2001). We explored different chain lengths and found that 5–10 million steps in the Markov chains with a burn-in period of 50 000 steps was sufficient to ensure convergence. We repeated every run five times with different seeds (to initialize the random number generator in the algorithm) to ensure convergence of the estimates. The method assumes the infinite-sites model of sequence evolution. Violations of the infinite-sites model occurred in our data. Removal of a single individual could resolve violations and thus enabled us to perform the test. An alternative solution is to remove sites that violate the infinite-sites assumption. We chose the former method.

Once we determined which populations were not isolated historically, we estimated gene flow among them by pairwise F_{ST} methods. For allozymes, pairwise F_{ST} values were estimated by Weir & Cockerham's (1984) θ-method using the DIST program (Slatkin 1993), and gene flow was estimated assuming $\hat{M} \approx (1/\theta - 1)/4$. For mitochondria, pairwise F_{ST} values were estimated from frequencies at polymorphic sites in DNA sequence data (Hudson *et al.* 1992), and gene flow was estimated assuming $\hat{M} \approx (1/F_{ST} - 1)/2$. Isolation-by-distance was assessed by testing the correlation of pairwise F_{ST} values and straight-line geographical distance (G) between vent localities. Mantel tests of the F_{ST} and G matrices were conducted with the R-package, using 1000 randomizations (Casgrain & Legendre 2000).

Results

Distribution

Bathymodiolus mussels are mid- to late-successional species at nascent eastern Pacific hydrothermal vents (Shank *et al.* 1998). They are often absent from new vents and highly disturbed areas. We searched for mussels at most of the EPR and GAR vent fields known to us during *Alvin*/*Atlantis* expeditions conducted between 1990 and 1999 (Fig. 1a; Table 1). No *Bathymodiolus* mussels have been observed in the 21° N latitude region of the EPR since the first visits in 1979, although other late-successional species such as the clam *Calyptogena magnifica* are abundant there (Speiss *et al.* 1980; Van Dover & Hessler 1990). The 21° N vent fields are north of the Rivera Fracture Zone (Fig. 1); however, it remains a mystery why clams have invaded this region and mussels have not (Van Dover 2000; p. 331). We also found no living mussels during six dives in the region between 18 and 21° S of the EPR during our expedition in 1999. Some mussel shell debris and many dead vestimentiferan tubeworms were observed at 20°03′ S latitude on the EPR. We suspect that the high rate of volcanic and tectonic activity in the 18–21° S region (Baker 1995) results in rapid habitat turnover that may not be conducive for establishment of robust *Bathymodiolus* colonies.

Mitochondrial DNA

We examined 689 bp of the mitochondrial COI gene from 120 individuals. Altogether, 41 COI haplotypes (GenBank Accession nos: AF456282–AF456322) were observed among these individuals. Nucleotide divergence between pairs of haplotypes ranged from 0.001 to 0.050 according to the K2P substitution model. A neighbour-joining tree

(Fig. 2) portraying the 41 COI haplotypes revealed two major lineages (I and II) that were separated by 17 fixed nucleotide substitutions. However, the differences between lineages I and II did not lead to any fixed amino acid substitutions according to a bivalve translation code (Hoffmann *et al.* 1992). Nonsynonymous substitutions occurred in some haplotypes (I → M at codon 8 for Bt20 and F → S at codon 82 for Bt28, Bt30 and Bt38). The average K2P distance between haplotypes belonging to lineages I and II was 0.045 (range: 0.039–0.050). Type I haplotypes could be subdivided into discrete subtypes (I-A and I-B, Fig. 2) that differed by 0.012 on average (range: 0.007–0.016). Type II haplotypes could be subdivided into two discrete subtypes (II-C and II-D, Fig. 2) that differed by 0.011 on average (range: 0.007–0.013).

The geographical distribution of mitochondrial haplotypes revealed two areas of regional differentiation in the eastern Pacific (Figs 1 and 2). First, the type I and II haplotypes segregated completely across the Easter Microplate. The type II lineages (Fig. 2) were only found in the 31–32° S region south of the Easter Microplate, whereas type I lineages occurred at all localities to the north. We subsequently refer to these two regions as SEM and NEM for south and north of the Easter Microplate, respectively. Second, a distinct shift in type I-A and I-B haplotype frequencies distinguished 17S from all other northern populations. The I-B subtype (blue in Fig. 1a) is absent at 17S. Average nucleotide divergence between pairs of populations ranged from 0.0048 to 0.0444 (Table 3). The number of fixed-differences ranged from 0 to 25 nucleotides. Pairwise χ^2 tests of differentiation revealed that the southern (SEM) populations were significantly different from all northern (NEM) populations (all *P*-values < 0.0027). In addition, the 17S population differed significantly from all other populations to the north (all *P*-values < 0.0252). Two southern hemisphere populations, 7S and 11S, had lower frequencies of the I-B subtype than GAR and all EPR populations north of the equator, but the differences were not statistically significant (Table 7). Frequencies of I-A and I-B haplotypes were essentially homogeneous among GAR and EPR populations north of the equator, as observed in the earlier study by Craddock *et al.* (1995).

Allozymes

We also examined allozymes encoded by nine polymorphic loci (Table 4). Genotypic frequencies generally conformed to random mating expectations within each population.

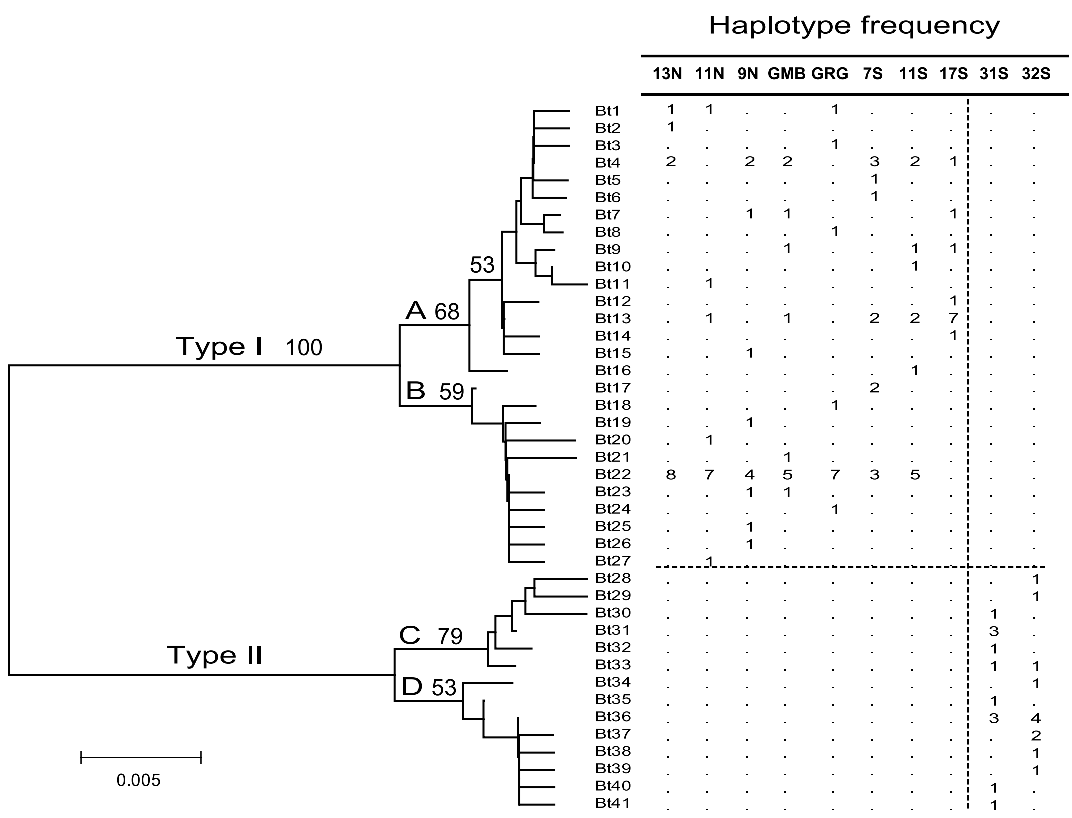

Fig. 2 Neighbour-joining (NJ) tree and frequencies of mitochondrial COI haplotypes from eastern Pacific *Bathymodiolus*. Bootstrap percentage values over 50% based on 100 replicates are indicated for the relevant branches.

Table 3 Average pairwise nucleotide divergence between populations (above diagonal), within populations (diagonal), and the number of fixed nucleotide differences (below diagonal) for mtCOI sequences

	13 N	11 N	9 N	GMB	GRG	7 S	11 S	17 S	31 S	32 S
13 N	0.0055	0.0052	0.0055	0.0056	0.0051	0.0059	0.0058	0.0072	0.0433	0.0440
11 N	0	0.0055	0.0056	0.0058	0.0050	0.0065	0.0062	0.0082	0.0433	0.0440
9 N	0	0	0.0063	0.0060	0.0055	0.0064	0.0062	0.0075	0.0437	0.0444
GMB	0	0	0	0.0065	0.0057	0.0061	0.0060	0.0067	0.0436	0.0442
GRG	0	0	0	0	0.0053	0.0064	0.0062	0.0081	0.0432	0.0439
7 S	0	0	0	0	0	0.0057	0.0055	0.0048	0.0429	0.0436
11 S	0	0	0	0	0	0	0.0060	0.0051	0.0432	0.0438
17 S	0	0	0	0	0	0	0	0.0014	0.0433	0.0440
31 S	22	21	22	22	21	20	22	24	0.0059	0.0058
32 S	23	22	23	23	22	21	23	25	0	0.0053

Most single-locus fixation indices (f_i) were close to 0 (no value was estimated if only a single heterozygote was found). Four f_i values of 59 tests were associated with significant heterozygote deficiencies (Table 4). After the application of a sequential Bonferroni correction (Rice 1989), no tests remained significant. Similarly, examination of multilocus F_{IS} values for each population (Table 4) revealed no significant overall heterozygote deficiencies. The overall mean F_{IS} was 0.046 and values ranged from −0.022 to 0.130. Although hermaphroditism has been reported for *B. thermophilus* (Berg 1985), no substantive evidence existed for deviations from random mating in our samples.

Significant geographical variances in allelic frequencies existed across the sampled range (Table 4). F_{ST} values at individual loci ranged from 0.016 to 0.645 with a multilocus mean of 0.230 ($\chi^2 = 855.4$, d.f. = 225, $P < 0.00001$). Significant F_{ST} values were found at five loci (*Aat-2*, *Idh-2*, *Lap*, *Pep-lgg* and *Pep-ll*). Most of the heterogeneity was due to divergence of the 31–32° S latitude (SEM) populations from all other populations to the north (NEM). Although no allozyme locus exhibited fixed differences between SEM and NEM populations, leading alleles at three loci were switched in SEM populations. Considering the NEM populations alone, the mean F_{ST} of 0.023 was small but still significant ($\chi^2 = 314.0$, d.f. = 175, $P < 0.001$). Exact tests for differentiation between pairs of NEM populations revealed significant differentiation between 17S and all populations to the north. The remaining NEM populations were relatively homogeneous, except for 11S, which differed slightly, but significantly, from GMB.

This multilocus pattern of divergence is best portrayed with a principal components analysis (Fig. 3). The first PCA axis is significant ($P = 0.001$) and accounts for 93.9% of the total variance (Fig. 3). The second axis captures 2.08% of the variance and is not significant ($P = 1.000$). Groups of populations that were not different based on exact tests of differentiation were encompassed by ellipses in Fig. 3. The first axis clearly portrays latitudinal shifts in allelic

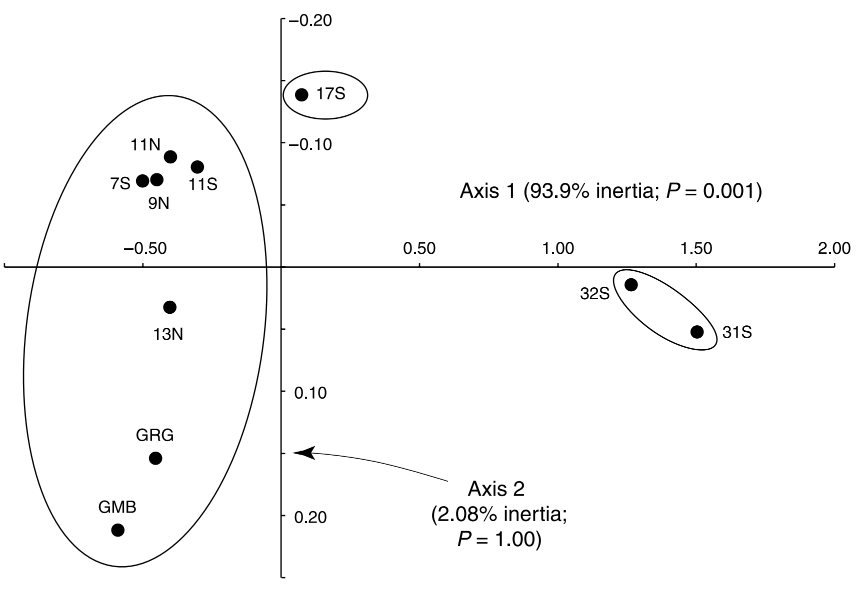

Fig. 3 Principal components analysis of nine allozyme loci.

Table 4 Allelic frequencies and *F*-statistics at nine allozyme loci

Locus, Allele	Locality 13N	11 N	9 N	GMB	GRG	7 S	11 S	17 S	31 S	32 S	F_{ST}†	(F_{ST}‡)
Aat											0.035*	(0.025)
A	0.000	0.000	0.000	0.000	0.000	0.019	0.000	0.000	0.033	0.000		
B	0.983	1.000	1.000	1.000	1.000	0.981	0.981	0.950	0.900	0.981		
C	0.000	0.000	0.000	0.000	0.000	0.000	0.019	0.050	0.067	0.019		
D	0.017	0.000	0.000	0.000	0.000	0.000	0.000	0.000	0.000	0.000		
f_i							–0.020	0.659*	–0.067			
Idh-2											0.516**	(0.06*)
A	0.190	0.080	0.086	0.023	0.075	0.063	0.222	0.300	0.950	0.926		
B	0.810	0.920	0.914	0.932	0.900	0.917	0.778	0.700	0.050	0.074		
C	0.000	0.000	0.000	0.023	0.025	0.021	0.000	0.000	0.000	0.000		
D	0.000	0.000	0.000	0.023	0.000	0.000	0.000	0.000	0.000	0.000		
f_i	0.231	–0.067	–0.077	–0.024	–0.063	–0.051	0.161	–0.094	–0.036	–0.061		
Lap											0.645**	(0.101**)
A	0.019	0.050	0.050	0.033	0.038	0.021	0.074	0.283	0.983	0.915		
B	0.981	0.950	0.950	0.967	0.962	0.979	0.926	0.717	0.017	0.185		
f_i		–0.036	–0.036	–0.018	–0.020		–0.061	–0.050		–0.209		
Mpi											0.016	(0.013)
A	0.017	0.033	0.017	0.043	0.000	0.043	0.019	0.000	0.000	0.019		
B	0.950	0.917	0.967	0.957	0.942	0.957	0.981	0.983	1.000	0.963		
C	0.033	0.050	0.017	0.000	0.058	0.000	0.000	0.017	0.000	0.019		
f_i	–0.024	–0.051	–0.009	–0.023	–0.042	–0.023				–0.010		
Opdh											0.016	(0.007)
A	0.017	0.000	0.017	0.019	0.019	0.000	0.019	0.017	0.017	0.000		
B	0.967	0.967	0.967	0.981	0.981	1.000	0.981	0.967	0.933	0.926		
C	0.017	0.033	0.017	0.000	0.000	0.000	0.000	0.017	0.050	0.074		
f_i	–0.009	–0.018	–0.009					–0.009	–0.040	–0.061		
Pep (lgg)											0.051**	(0.030*)
A	0.034	0.034	0.050	0.054	0.042	0.032	0.074	0.050	0.050	0.019		
B	0.190	0.172	0.150	0.250	0.250	0.161	0.204	0.233	0.417	0.315		
C	0.052	0.052	0.200	0.071	0.042	0.016	0.056	0.000	0.000	0.000		
D	0.448	0.414	0.317	0.518	0.563	0.452	0.333	0.317	0.150	0.204		
E	0.052	0.000	0.050	0.000	0.000	0.016	0.037	0.000	0.000	0.000		
F	0.224	0.310	0.233	0.107	0.104	0.323	0.278	0.400	0.383	0.444		
G	0.000	0.017	0.000	0.000	0.000	0.000	0.019	0.000	0.000	0.019		
f_i	0.090	–0.019	0.245*	–0.026	0.060	–0.003	0.044	0.041	0.151	0.011		
Pep (ll)											0.124**	(0.033*)
A	0.000	0.000	0.000	0.000	0.000	0.031	0.000	0.000	0.000	0.000		
B	0.018	0.052	0.052	0.000	0.043	0.000	0.037	0.000	0.000	0.000		
C	0.500	0.362	0.466	0.640	0.391	0.469	0.444	0.300	0.017	0.130		
D	0.446	0.569	0.448	0.360	0.543	0.406	0.370	0.600	0.933	0.852		
E	0.018	0.017	0.034	0.000	0.022	0.094	0.148	0.100	0.050	0.019		
F	0.018	0.000	0.000	0.000	0.000	0.000	0.000	0.000	0.000	0.000		
f_i	0.173	0.000	0.064	0.152	0.072	0.035	–0.077	0.275	–0.040	0.154		
Pgdh-1											0.031	(0.051*)
A	0.000	0.000	0.000	0.000	0.000	0.000	0.000	0.000	0.017	0.000		
B	0.000	0.000	0.000	0.000	0.000	0.056	0.000	0.000	0.000	0.019		
C	1.000	1.000	1.000	1.000	1.000	0.944	1.000	1.000	0.983	0.981		
f_i						–0.030						
Gpi											0.021	(0.022)
A	0.017	0.000	0.033	0.000	0.000	0.000	0.019	0.067	0.017	0.000		
B	0.967	0.967	0.950	0.983	1.000	1.000	0.981	0.917	0.967	1.000		
C	0.017	0.033	0.017	0.017	0.000	0.000	0.000	0.017	0.017	0.000		
f_i	–0.009	–0.018	0.322*					–0.058	0.500*		Means	(Means)
F_{IS}	0.119	–0.022	0.130	0.030	0.034	0.000	0.017	0.070	0.081	–0.016	0.046	(0.050)

F_{ST} = the mean standardized variance; H_O = observed multilocus heterozygosity; H_E = Nei's (1978) unbiased estimate of expected heterozygosity; and $F_{IS} = 1 - (H_O/H_E)$.
†Including 31–32 S populations.
‡Excluding 31–32 S populations.
Significance at *α = 0.05 level, and **α = 0.01, respectively. Prior to Bonferroni corrections.

frequencies, effectively separating populations north and south of the Easter Microplate. The 17S population is separated from the other NEM populations, a reflection of intermediate allelic frequencies at several loci. It is worth noting that axis 2 separates the Galapagos populations from other NEM populations; however, the axis does not explain a significant component of the variance in allelic frequencies.

Gene diversity

The diversities of allozymes and mtDNA were compared across the 10 populations (Table 5). Mean heterozygosity for allozymes (H_E) was highest at 17S ($H_E = 0.271$) and significantly higher (Wilcoxan sign-rank test, $P = 0.002$) than the combined mean of the remaining nine populations (0.191 ± 0.009). In contrast, nucleotide diversity (π) was lowest at 17S ($\pi = 0.0014$) and significantly lower (Wilcoxan sign-rank test, $P = 0.002$) than the mean of the remaining populations (0.0057 ± 0.0014). Nucleotide diversity and allozyme diversity were negatively correlated ($r = -0.7016$; $P = 0.0237$), but the relationship was entirely due to 17S. When 17S was excluded from the analysis, H_E and π were no longer correlated. Haplotype diversity ($\hat{H}$) of mtDNA also varied considerably among populations and was highest at 31S.

Isolation test

We tested the assumption of ongoing gene flow using the mitochondrial data and a method recently developed by Nielsen & Wakeley (2001). To facilitate analyses with this computationally intensive method, we pooled populations that were effectively identical based on mtDNA and allozyme analyses into the following groups: 9° N–13° N (NEPR); GMB and GRG (GAR); and 31° S–32° S (SEM). No evidence existed for subdivision within these groups, and each group was restricted to a single ridge segment, or to contiguous segments. The remaining populations (7, 11 and 17S) were not pooled because they occupied ridge segments separated by large offsets (> 100 km). An analysis of molecular variance (AMOVA) of the mitochondrial data revealed that interpopulational variance within the pooled groups explained only 0.53% of the total variance, an insignificant variance component ($P = 0.2687$).

We were able to reject the hypothesis of complete isolation between all pairs of populations (or groups of populations) north of the Easter Microplate (Table 6). However, we did not reject the isolation hypothesis between the NEM and SEM. Pairwise maximum likelihood estimates (MLEs) of $\hat{M}$, likelihood ratio test statistics, and their P-values for the mitochondrial data are presented in Table 6. We found

Table 5 Genetic variability of allozymes and mitochondrial COI

	Allozyme					mtDNA COI			
Population	$\bar{N}$ (SE)	$\bar{A}$ (SE)	P	$\bar{H}_O$ (SE)	$\bar{H}_E$ (SE)	N	H	π (SE)	$\hat{H}$ (SE)
13 N	29.0 (0.4)	3.0 (0.5)	88.9	0.185 (0.076)	0.210 (0.087)	12	4	0.0054 (0.0012)	0.561 (0.154)
11 N	29.2 (0.5)	2.6 (0.5)	77.8	0.204 (0.086)	0.200 (0.085)	12	6	0.0055 (0.0016)	0.682 (0.148)
9 N	29.8 (0.1)	2.8 (0.5)	77.8	0.180 (0.077)	0.207 (0.094)	12	8	0.0063 (0.0011)	0.894 (0.078)
GMB	26.3 (1.0)	2.3 (0.4)	77.8	0.160 (0.077)	0.165 (0.079)	12	7	0.0064 (0.0009)	0.833 (0.100)
GRG	24.9 (0.7)	2.3 (0.5)	66.7	0.171 (0.076)	0.177 (0.081)	12	6	0.0052 (0.0016)	0.682 (0.148)
7 S	25.4 (1.4)	2.6 (0.5)	77.8	0.191 (0.086)	0.191 (0.088)	12	6	0.0057 (0.0007)	0.879 (0.060)
11 S	27.0 (0.0)	2.7 (0.6)	88.9	0.230 (0.098)	0.234 (0.098)	12	6	0.0059 (0.0006)	0.818 (0.096)
17 S	30.0 (0.0)	2.4 (0.3)	88.9	0.252 (0.081)	0.271 (0.085)	12	6	0.0014 (0.0004)	0.682 (0.148)
31 S	30.0 (0.0)	2.6 (0.3)	88.9	0.137 (0.058)	0.149 (0.067)	12	8	0.0058 (0.0007)	0.909 (0.065)
32 S	27.0 (0.0)	2.4 (0.4)	88.9	0.189 (0.071)	0.186 (0.070)	12	8	0.0053 (0.0013)	0.894 (0.078)

$\bar{N}$ = mean sample size per locus; (SE) = standard error; $\bar{A}$ = mean number of alleles per locus; P = percentage of polymorphic loci; $\bar{H}_O$ = mean heterozygosity per locus by direct count; $\bar{H}_E$ = mean heterozygosity assuming Hardy–Weinberg equilibrium; N = sample number of sequences; H = number of haplotypes; π = nucleotide diversity; $\hat{H}$ = haplotype diversity.

Table 6 Log-likelihood ratio test for migration vs. isolation. Above diagonal: likelihood ratio test statistics with P-value in parenthesis (italics). Below diagonal: maximum likelihood estimate of migration rate based on mitochondrial DNA, and (in parens) F_{ST}-based estimates for mtDNA and allozymes, respectively

	NEPR	GAR	7 S	11 S	17 S	SEM
NEPR		10.84 *(0.0005)*	5.03 *(0.0124)*	13.08 *(0.0001)*	15.21 *(0.0001)*	0 *(0.5000)*
GAR	> 100 (undef, 18.75)		5.34 *(0.0104)*	13.54 *(0.0001)*	15.20 *(0.0001)*	0 *(0.5000)*
7 S	2.4 (4.57, 83.6)	2.6 (5.45, 16.59)		10.16 *(0.0007)*	5.45 *(0.0098)*	0 *(0.5000)*
11 S	49.4 (20.30, 44.67)	51.8 (25.04, 7.28)	35.2 (undef, 36.16)		7.52 *(0.0031)*	0 *(0.5000)*
17 S	0.68 (0.39, 4.34)	0.98 (0.42, 2.19)	0.56 (1.47, 3.47)	2.76 (1.08, 9.04)		0 *(0.5000)*
SEM	< 0.01 (0.06, 0.27)	< 0.01 (0.06, 0.21)	< 0.01 (0.06, 0.22)	< 0.01 (0.07, 0.30)	< 0.01 (0.04, 0.53)	

three general classes of likelihood curves for $\hat{M}$ based on the mitochondrial data (Fig. 4). Comparisons involving GAR are not illustrated, because they were qualitatively similar to results obtained with NEPR comparisons. In all cases that failed to reject the null hypothesis of isolation (H_O: $\hat{M} = 0$), likelihood curves decreased sharply as a function of increasing $\hat{M}$ (Fig. 4a). All comparisons involving SEM generated this type of curve. These curves are qualitatively similar to those obtained from simulations with $M = 0$ (Nielsen & Wakeley 2001). Although we cannot rule out extremely low levels of gene flow involving SEM populations, we have excluded SEM from further analyses of gene flow (below), as it appears to be effectively isolated from the northern populations. Likelihood curves from comparisons involving the 17S population (Fig. 4b) have maxima near $\hat{M}$ 1. These curves are qualitatively similar to those obtained with simulated data assuming $M = 1$ (Nielsen & Wakeley 2001). Comparisons involving the northern groups of populations (Fig. 4c) produced flat curves, a consequence of very high rates of gene flow. Maxima estimated from these flat curves were not robust; however, we can confidently reject low values of $\hat{M}$.

Gene flow

F_{ST}-based methods for estimating gene flow assume that populations are at equilibrium between gene flow and genetic drift. This assumption is violated if populations are historically isolated. High levels of variation within the isolated populations generate F_{ST} values < 1 and estimates of $\hat{M} > 0$, even if the populations share no alleles (Neigel 1997; Hedrick 1999). Nonzero rates of gene flow would also be mistakenly inferred from genes that retain ancestral polymorphisms after isolation is complete, as is often true for allozymes, which coalesce more slowly than mitochondrial polymorphisms. Finally, balancing selection acting on allozymes (e.g. Karl & Avise 1992) would upwardly bias estimates of $\hat{M}$. Thus, it is not surprising that our allozyme-based estimates of $\hat{M}$ exceeded the mitochondria-based estimates for population pairs that are completely isolated (SEM vs. all NEM) or share low level of gene flow (17S vs. all other NEM) (Table 6). The two mitochondrial estimators of $\hat{M}$ (MLE and F_{ST}, Table 6) were highly correlated (Mantel test: $r = 0.9035$; $P = 0.0012$). Both were calculated from the same subset of data from which we removed samples that violated the infinite-sites model. The F_{ST}-based estimates of $\hat{M}$ from allozymes were only marginally correlated with those estimated from mtDNA (Mantel test: $r = 0.724$; $P = 0.0519$).

For the NEM populations alone, we tested dispersal models using the isolation-by-distance method of Slatkin (1993). Under the null hypothesis (i.e. the island model), no relationship should exist between divergence (F_{ST}) and geographical distance, whereas a positive relationship is expected under isolation-by-distance or stepping-stone models of dispersal. Both mtDNA (Mantel test: $r = 0.533$, $P = 0.003$) and allozyme data (Mantel test: $r = 0.498$, $P = 0.001$) provided evidence for isolation-by-distance (Fig. 5); however, the regression slopes differed by an order of magnitude. Exclusion of the 17S sample resulted in no significant correlation for mtDNA (Mantel test: $r = 0.411$; $P = 0.092$), but a slight correlation remained for allozymes (Mantel test: $r = 0.379$; $P = 0.041$).

Discussion

Our analysis of *Bathymodiolus* mussels from hydrothermal vents along the East Pacific Rise and Galapagos Rift revealed three conspicuous components of genetic structure. First, the northern groups of populations, spanning 13° N to 11° S latitude on the East Pacific Rise and the Galapagos Rift, were relatively homogenous genetically. Second,

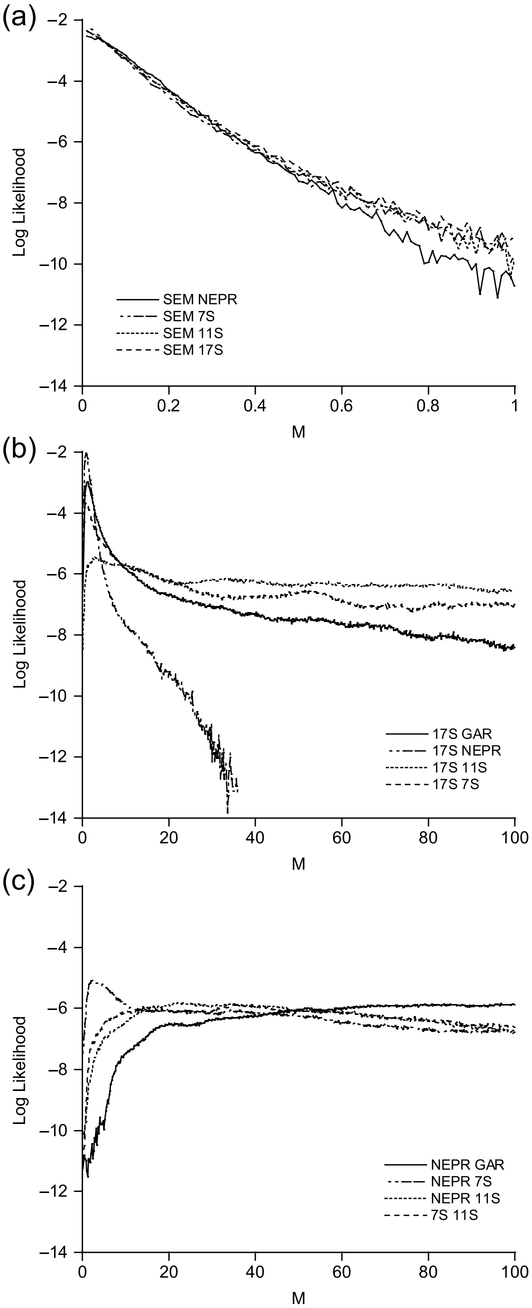

Fig. 4 Likelihood curves for $\hat{M}$ estimated from the mitochondrial COI sequences: (a) SEM vs. all other populations (parameters: $M_{max} = 5$, $T_{max} = 20$); (b) 17S vs. other northern populations (parameters: $M_{max} = 100$, $T_{max} = 5$); and (c) comparisons of NEPR, GAR and SEPR populations that had flat curves (parameters: $M_{max} = 100$, $T_{max} = 5$).

populations found north and south of the Easter Microplate region were highly divergent and isolated with respect to gene flow. Third, the 17S population was partially isolated from all other populations to the north. We consider below topographic and hydrographic factors that might affect population structure within and between these regions.

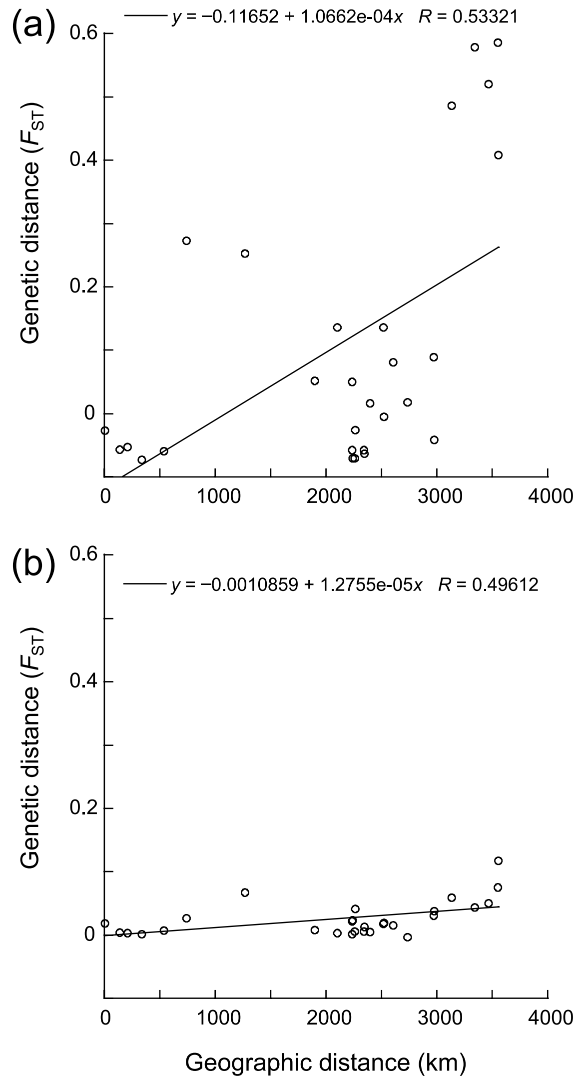

Fig. 5 Relationships between geographical distance and pairwise genetic distances from (a) mitochondrial COI sequences and (b) multilocus allozymes.

Homogeneity in the northern region

Craddock *et al*. (1995) previously reported that *Bathymodiolus thermophilus* populations from the northern East Pacific Rise and the Galapagos Rift are relatively homogenous, showing no evidence for isolation-by-distance throughout this portion of their range. Our results revealed that this region of relative genetic homogeneity extends south of the equator to 11° S latitude on the EPR. It should be noted that this region of the EPR crosses several long transform faults (e.g. Clipperton, Siqueros, Quebrada, Wilkes, Fig. 1a) that seem to have no significant effect on rates of gene flow. High rates of gene flow across this region, generally more than five migrants per generation (Table 7), may be facilitated by the homogeneity of bathymetry and deep ocean currents in this region. Direct measurements of deep-bottom currents were recorded at 13° N over a four-month period (Chevaldonné *et al*. 1997), and at 9°50′ N for about one year (Marsh *et al*. 2001). A long-term flow regime alternates primarily between NNW and SSE directions along the ridge axis, although semidiurnal periodicity generates east–west currents and considerable variability in current velocity. These primary vectors, however, will tend to transport larvae along the axis of the ridge system, although it remains unclear how larvae move to and from Galapagos vent localities that are 2000 km east of the EPR.

The Easter Microplate boundary

Bathymodiolus populations from south of the Easter Microplate (SEM = 31 and 32S) differed significantly from all other populations to the north (NEM). Average pairwise sequence divergence for mitochondrial COI was 4.4%, and the haplotype tree (Fig. 2) showed reciprocal monophyly of type I (NEM) and type II (SEM) haplotypes. This level of divergence greatly exceeds the maximum divergence (0.82%) among NEM populations spread across 3500 km north of the Easter Microplate. Significant shifts in allozyme frequencies also existed between SEM and NEM, although no fixed differences were observed. Allozyme distance (Nei's *D*) between regions was 0.242, which also greatly exceeded the maximum *D* (0.035) among NEM populations.

Levels of mitochondrial and allozyme divergence between mussels from the two regions (NEM and SEM) suggest that they warrant consideration as distinct species. Although the criteria for erecting new species are diverse, as are species concepts (Mayden 1997), concordant divergence across multiple gene loci provides a useful indicator of historical isolation and, thus, an operational criterion for recognizing species boundaries (Avise & Wollenberg 1997). Allozyme distance between NEM and SEM groups exceeds the distance between *Bathymodiolus azoricus* and *B. puteoserpentis* ($D = 0.112$), parapatric sibling-species from the Mid-Atlantic Ridge (Maas *et al*. 1999; O'Mullan *et al*. 2001). Morphological comparisons of NEM and SEM mussels are incomplete, but basic conchological measurements (as in Maas *et al*. 1999) revealed no obvious differences between them. We recognize *Bathymodiolus* mussels from north of the Easter Microplate (NEM) as *B. thermophilus sensu strictu* (type locality, Mussel Bed, Galapagos Rift, Kenk & Wilson 1985). To adequately assess the evolutionary integrity of SEM mussels, we will need additional samples from the Easter Microplate region and from more regions to the south.

Isolation of these putative species may be coincident with evolution of the Easter Microplate, a topographically inflated feature that disrupts the linear structure of the southern East Pacific Rise (Naar & Hey 1991). This small tectonic plate is surrounded on the north and south by transform faults, and on the east and west by a broad chain of young seamounts comprising the East and West Rifts (Searle *et al*. 1989). The seamounts formed by rift

Table 7 Proportion of genetic diversity found between pairs of populations (F_{ST}, below diagonal) and corresponding estimate of gene flow ($\hat{M}$, above diagonal) from multilocus allozymes and mtDNA

Locality	13 N	11 N	9 N	GMB	GRG	7 S	11 S	17 S
F_{ST} and $\hat{M}$ from multilocus allozymes								
13 N		59.61	145.37	18.76	41.29	177.47	undef	4.74
11 N	0.004		78.97	5.86	42.43	70.37	15.86	5.48
9 N	0.002	0.003		10.32	11.31	30.55	48.39	3.97
GMB	0.013	**0.041**	0.024		13.39	12.74	6.38	1.87
GRG	0.006	0.006	0.022	0.018		13.92	7.91	3.09
7 S	0.001	0.004	0.008	0.019	0.018		36.16	3.47
11 S	−0.003	0.016	0.005	**0.038**	0.031	0.007		9.04
17 S	**0.050**	**0.044**	**0.059**	**0.118**	**0.075**	**0.067**	0.027	
F_{ST} and $\hat{M}$ from mtDNA								
13 N		undef	undef	undef	undef	9.468	27.586	0.462
11 N	−0.057		undef	undef	undef	3.182	5.640	0.366
9 N	−0.073	−0.053		undef	undef	9.118	31.358	0.530
GMB	−0.063	−0.026	−0.071		undef	undef	undef	0.726
GRG	−0.058	−0.071	−0.058	−0.027		3.186	5.112	0.352
7 S	0.050	**0.136**	0.052	−0.005	0.136		undef	1.472
11 S	0.018	0.081	0.016	−0.041	0.089	−0.059		1.328
17 S	**0.520**	**0.578**	**0.486**	**0.408**	**0.586**	**0.253**	**0.273**	

Bold case indicates significant value ($\alpha = 0.05$) based on exact test (Goudet *et al*. 1996).

propagation (Hey 1977), beginning ≈ 4.5 Ma when the East Rift started to propagate northward (Naar & Hey 1991). If we assume, based on comparative evidence (Knowlton 1993), that mtCOI sequences diverged at a rate of ≈ 1.0–2.0% per Myr, the SEM and NEM groups separated 2.1–4.3 Ma, which is consistent with formation of the Easter Microplate. However, estimates of divergence dates based on a comparative molecular clock are subject to large errors and are particularly sensitive to the assumption that divergence rates for a particular gene are homogeneous across divergent taxa (Hillis *et al*. 1996). Clearly, it would be desirable to identify independent criteria for calibrating a molecular clock specific to deep-sea mussels.

Allopatric divergence across the Easter Microplate could accumulate from a combination of neutral processes and diversifying selection between physically or biologically divergent regions. Application of the isolation test (Nielsen & Wakeley 2001) to our mitochondrial data indicated that little to no contemporary gene flow exists between mussel populations on either side of the Easter Microplate. Mitochondrial variation exhibited a rectilinear step cline between the two regions, but frequency shifts in allozymes varied from steep to flat. Nevertheless, 93.9% of the multilocus variance in allozyme frequencies could be explained by a cline that covaried with distance along the East Pacific Rise (Fig. 3). Based on slopes of the allozyme clines, and the logic employed by Barton (1983), we might hypothesize that spatially diversifying selection acts most stringently on mtDNA haplotypes, followed by allozymes, in the order: *Lap*, *Idh-2*, *Pep-ll*, *Pep-lgg* and *Aat*. Four other allozyme loci with limited polymorphism were not clinal. *Lap* polymorphism in the near shore mussel, *Mytilus edulis*, is well known for reflecting differential selection across salinity gradients (Koehn *et al*. 1980; Gardner & Kathiravetpillai 1997). The *Lap* locus also exhibits a cline between *B. azoricus* and *B. puteoserpentis*, which hybridize at an intermediate locality on the Mid-Atlantic Ridge (O'Mullan *et al*. 2001). Diversifying selection is plausible in the mid-Atlantic mussels, because the shallow vs. deep bathymetric regimes occupied by two species differ in geochemical milieu (Desbruyères *et al*. 2000a,b). Nevertheless, we have no reason to believe that regions north and south of the Easter Microplate should generate distinct selective regimes. Depths of vent habitats are similar (2500 ± 250 m) in the two regions, and temperatures of vent effluents overlap broadly, as do the concentrations of chloride, hydrogen sulphide, and iron (D. Butterfield, pers. commum.).

Bathymodiolus mussels possess free-swimming, feeding (i.e. planktotrophic) larvae capable of long-distance dispersal, although it is not known how high they rise in the water column (Lutz *et al*. 1979, 1980). Certainly, genetic homogeneity of mussel populations from 13° N to 11° S on the EPR and the Galapagos Rift is indicative of high dispersal rates. Nevertheless, we hypothesize that dispersing larvae can be removed from the vicinity of the ridge system by strong cross-axis currents in other regions to the south. Few direct studies of currents have been conducted in the remote region of the Easter Microplate, but general circulation patterns have been inferred from computer simulations based on a robust model of deep-ocean circulation at 2000–3000 m depth (Fujio & Imasato 1991). Accordingly, a strong anticyclonic (westward) circulation exists along the northern flank of the Easter Microplate at 22–25° S (Fig. 1a,b). This hypothesized gyre of the Antarctic circumpolar current (ACC) is induced by inflated bottom topography along the walls of the ridge axis. Additionally, the shallow bathymetry associated with young seamounts propagating east and west of the microplate may accentuate cross-axis circulation. In contrast, a strong cyclonic (eastward) circulation was proposed for this region in an earlier study based on different assumptions about barotropic flow across the EPR (see Fig. 50 in Reid 1986). Despite opposing conclusions about the direction of flow, both studies propose a strong cross-axis current in the region of the Easter Microplate. Thus, the larvae of vent species that feed and develop high in the water column, and those that disperse in buoyant hydrothermal plumes (Mullineaux *et al*. 1995), are likely to be removed from the axis. In contrast, species with negatively buoyant propagules and arrested development are more likely to be retained (Pradillon *et al*. 2001). Acting together, deep oceanic currents and topographical features of the ridge system contribute to geographical subdivision of East Pacific Rise (EPR) populations of *Bathymodiolus* mussels and possibly other hydrothermal vent invertebrates.

Partial isolation of the 17° S region

A weaker dispersal barrier occurs north of the Easter Microplate in the region between 11 and 17° S latitude. A common mtCOI haplotype in NEM populations (I-B, coloured blue in Fig. 1a) was absent at 17S, and multilocus allozyme data separated 17S from NEM populations to the north (Fig. 3). Pairwise estimates of gene flow involving 17S were generally much lower than rates found among populations to the north (Table 6). We hypothesize that restricted gene flow between 17S and all other NEM populations results from a strong westward current that crosses the ridge axis around 15° S latitude. Elevated He-3 concentrations mark buoyant hydrothermal plumes along the EPR. A survey of He-3 plumes in this region revealed a strong westward flow centred at 15° S (Lupton & Craig 1981; Lupton 1998). Fujio & Imasato (1991) conclude that the westward distribution of He-3 in this region may be caused by the strong anticyclonic circulation in the southern East Pacific (Fig. 1b,c). If *B. thermophilus* larvae disperse in buoyant plumes, they would be less likely to traverse a region of cross-axis currents.

Estimates of genetic diversity based on mtCOI and allozymes were at odds with respect to the 17S population (Table 5). Nucleotide diversity in mtCOI was lowest at 17S and allozyme diversity was highest. Mitochondrial variation could decrease quickly because of metapopulation processes in this highly unstable region. The area from 13 to 20° S latitude is one of the fastest spreading regions of the global mid-ocean ridge system. This area is subject to frequent volcanism and rapid habitat turnover (Baker & Urabe 1996; Embley *et al*. 1998), and the resulting local extinctions and recolonization events could quickly erode mitochondrial diversity. Although allozymes experience the same metapopulation processes, they are more likely than mitochondria to retain diversity. Coalescence time is expected to be shorter for mitochondrial variants, because effective population size of a maternally transmitted gene should be one-fourth that of a comparable nuclear gene in a diploid species (Birky *et al*. 1983). Nevertheless, it should be noted that doubly uniparental inheritance (DUI) of gender-specific mitochondrial lineages occurs in some mytilids (Skibinski *et al*. 1994; Zouros *et al*. 1994), potentially altering expectations of variance-effective size. However, the variant mitochondrial types seen in *B. thermophilus* are not associated with gender (Maas *et al*. in preparation). Examination of nuclear gene sequences from the 17S region might help to clarify the apparent discrepancy between allozyme and mitochondrial diversities. For example, we cannot exclude historical intergradation between NEM and SEM mussels. Hybridization occurs between similarly divergent mussel species along the Mid-Atlantic Ridge (O'Mullan *et al*. 2001).

Additional samples from the Easter Microplate region, the Juan Fernandez Microplate, and southward along the Pacific Antarctic Ridge are needed to assess our hypothesis that an interaction between ridge topography and cross-axis currents disrupts dispersal of vent larvae across this volcanically and tectonically dynamic region. Observations in the 17S region of novel species not previously seen to the north (e.g. a *Chorocaris* shrimp and an *Eosipho* snail) suggests that this region might represent a boundary between northern and southern EPR subprovinces (C.L. Van Dover, pers. commun.). This boundary lies at the interface between the major Indo-Pacific and Antarctic zoogeographical divisions (Vinogradova 1979). Comparative phylogeographical studies of other vent-endemic species should verify whether the currently hypothesized barriers are dominant physiographic features in this southernmost region of the East Pacific Rise.

Acknowledgements

We thank the crew and pilots of the *R/V Atlantis* and the *DSV Alvin* for their significant efforts and technical support. We also thank the scientists aboard *R/V Atlantis* during the SEPR'99 cruise, and particularly J. Lupton, D. Butterfield and R. Hey, for critical insights regarding geological and chemical processes. Dr S. Fujio kindly provided the information on deep ocean circulation data. Our colleague, Peter Smouse, provided helpful recommendations regarding statistical analyses. Funding for this project was provided by the Monterey Bay Aquarium Research Institute (The David and Lucile Packard Foundation), the New Jersey Agricultural Experiment Station, and NSF grant OCE9910799.

References

Avise JC, Wollenberg K (1997) Phylogenies and the origin of species. *Proceedings of the National Academy of Sciences of the USA*, **94**, 7748–7755.

Baker ET (1995) Characteristics of hydrothermal discharge following a magmatic intrusion. In: *Hydrothermal Vents and Processes* (eds Parson LM, Walker CL, Dixon, DR), pp. 65–76. The Geological Society, London.

Baker ET, Urabe T (1996) Extensive distribution of hydrothermal plumes along the superfast spreading East Pacific Rise, 13°30′–18°40′ S. *Journal of Geophysical Research, B, Solid Earth and Planets*, **101**, 8685–8695.

Barton NH (1983) Multilocus clines. *Evolution*, **37**, 454–471.

Berg CJ Jr (1985) Reproductive strategies of mollusks from abyssal hydrothermal vent communities. *Biological Society of Washington Bulletin*, **6**, 185–197.

Birky CWJ, Maruyama T, Fuerst P (1983) An approach to population and evolutionary genetic theory for genes in mitochondria and chloroplasts, and some results. *Genetics*, **103**, 513–527.

Casgrain P, Legendre P (2000) *The R Package for Multivariate and Spatial Analysis,* Version 4.0. *(Development Release 2)*. University of Montréal, Montréal, Canada.

Chevaldonné P, Jollivet D, Vangrieshiem A, Desbruyères D (1997) Hydrothermal-vent alvinellid polychaete dispersal in the eastern Pacific. 1. Influence of vent site distribution, bottom currents, and biological patterns. *Limnology and Oceanography*, **42**, 67–80.

Craddock C, Hoeh WR, Lutz RA, Vrijenhoek RC (1995) Extensive gene flow in the deep-sea hydrothermal vent mytilid *Bathymodiolus thermophilus*. *Marine Biology*, **124**, 137–146.

Desbruyères D, Almeida A, Comtet T *et al.* (2000a) A review of the distribution of hydrothermal vent communities along the northern Mid-Atlantic Ridge: dispersal vs. environmental controls. *Hydrobiologia*, **440**, 201–216.

Desbruyères D, Biscoiti M, Caprais J-C *et al.* (2000b) Variations in deep-sea hydrothermal vent communities on the Mid-Atlantic ridge near the Azores plateau. *Deep Sea Research*, **I** (48), 1325–1346.

Doyle JJ, Dickson E (1987) Preservation of plant samples for DNA restriction endonuclease analysis. *Taxon*, **36**, 715–722.

Embley RW, Lupton JE, Massoth G *et al.* (1998) Geological, chemical, and biological evidence for recent volcanism at 17.5° S: East Pacific Rise. *Earth and Planetary Science Letters*, **163**, 131–147.

Fisher CR, Childress JJ, Brooks JM, Macko SA (1994) Nutritional interactions in Galapagos Rift hydrothermal vent communities: inferences from stable carbon and nitrogen isotope analyses. *Marine Ecology Progress Series*, **103**, 45–55.

Folmer O, Black M, Hoeh W, Lutz R, Vrijenhoek R (1994) DNA primers for amplification of mitochondrial cytochrome C oxidase subunit I from metazoan invertebrates. *Molecular Marine Biology and Biotechnology*, **3**, 294–299.

Fujio S, Imasato N (1991) Diagnostic calculation for circulation and water mass movement in the deep pacific. *Journal of Geophysical Research*, **96**, 759–774.

Gage JD, Tyler PA (1991) *Deep Sea Biology: A Natural History of Organisms at the Deep-Sea Floor*. Cambridge University Press, Cambridge.

Gardner JPA, Kathiravetpillai G (1997) Biochemical genetic variation at a leucine aminopeptidase (LAP) locus in blue (*Mytilus galloprovincialis*) and Greenshell (*Perna canaliculus*) mussel populations along a salinity gradient. *Marine Biology*, **128**, 619–625.

Goudet J (1999) *PCAGEN for Windows*, Version 1.2. University of Lausanne, Lausanne, Switzerland.

Goudet J, Raymond M, DeMee ST, Rousset F (1996) Testing differentiation in diploid populations. *Genetics*, **144**, 1933–1940.

Grassle JF (1985) Hydrothermal vent animals: distribution and biology. *Science*, **229**, 713–717.

Hebert PDN, Beaton M (1989) *Methodologies for Allozyme Analysis Using Cellulose Acetate Gels*. Helena Laboratories, Beaumont, TX.

Hedrick PW (1999) Perspective: highly variable loci and their interpretation in evolution and conservation. *Evolution*, **53**, 313–318.

Hey RN (1977) A new class of pseudofaults and their bearing on plate tectonics: a propagating rift model. *Earth and Planetary Science Letters*, **37**, 321–325.

Hey J, Wakeley J (1997) A coalescent estimator of the population recombination rate. *Genetics*, **145**, 833–846.

Hillis DM, Mable BK, Moritz C (1996) Applications of molecular systematics: the state of the field and a look to the future. In: *Molecular Systematics* (eds Hillis DM, Moritz C, Mable, BK), pp. 515–543. Sinauer Associates, Sunderland, MA.

Hoffmann RJ, Boore JL, Brown WM (1992) A novel mitochondrial genome organization for the blue mussel, *Mytilus edulis*. *Genetics*, **131**, 397–412.

Hudson RR, Slatkin M, Maddison WP (1992) Estimation of levels of gene flow from DNA sequence data. *Genetics*, **132**, 583.

Jollivet D, Chevaldonné P, Planque B (1999) Hydrothermal-vent alvinellid polychaete dispersal in the Eastern Pacific. 2. A metapopulation model based on habitat shifts. *Evolution*, **53**, 1143–1156.

Karl SA, Avise JC (1992) Balancing selection at allozyme loci in oysters: implications from nuclear RFLPs. *Science*, **256**, 100–102.

Kenk VC, Wilson BR (1985) A new mussel (Bivalvia, Mytilidae) from hydrothermal vents in the Galapagos Rift zone. *Malacologia*, **26**, 253–271.

Kim S, Mullineaux LS (1998) Distribution and near-bottom transport of larvae and other plankton at hydrothermal vents. *Deep Sea Research*, **II** (45), 423–440.

Kimura M (1980) A simple method for estimating evolutionary rates of base substitution through comparative studies of nucleotide sequences. *Journal of Molecular Evolution*, **16**, 111–120.

Knowlton N (1993) Sibling species in the sea. *Annual Review of Ecology and Systematics*, **24**, 189–216.

Koehn RK, Newell RIE, Immerman F (1980) Maintenance of an aminopeptidase allele frequency cline by natural selection. *Proceedings of the National Academy of Sciences of the USA*, **77**, 5385–5389.

Kumar S, Tamura K, Nei M (1994) MEGA: molecular evolutionary genetics analysis software for microcomputers, v. 1.01. *CABIOS*, **10**, 189–191.

Lupton JE (1998) Hydrothermal helium plumes in the Pacific Ocean. *Journal of Geophysical Research-Oceans*, **103**, 15853–15868.

Lupton JE, Craig H (1981) A major helium-3 source at 15° S on the East Pacific Rise. *Science*, **214**, 13–18.

Lutz RA, Jablonski D, Rhoads DC, Turner RD (1980) Larval dispersal of a deep-sea hydrothermal vent bivalve from the Galapagos Rift. *Marine Biology*, **57**, 127–133.

Lutz RA, Rhoads DC, Jablonski D, Turner RD (1979) High larval dispersal capability of a deep-sea hydrothermal vent bivalve from the Galapagos Rift. *American Zoologist*, **19**, 927.

Maas PAY, O'Mullan GD, Lutz RA, Vrijenhoek RC (1999) Genetic and morphometric characterization of mussels (Bivalvia: Mytilidae) from Mid-Atlantic hydrothermal vents. *Biological Bulletin*, **196**, 265–272.

Marsh AG, Mullineaux LS, Young CM, Manahan DT (2001) Larval dispersal potential of the tubeworm *Riftia pachyptila* at deep-sea hydrothermal vents. *Nature*, **411**, 77–80.

Mayden RL (1997) A hierarchy of species concepts: the denouement in the saga of the species problem. In: *Species: the Units of Biodiversity* (eds Claridge MF, Dawah HA, Wilson MR), pp. 381–424. Chapman & Hall, London.

Mullineaux LS, Weibe PH, Baker ET (1995) Larvae of benthic invertebrates in hydrothermal vent plumes over the Juan de Fuca Ridge. *Marine Biology*, **122**, 585–596.

Naar DF, Hey RN (1991) Tectonic evolution of the Easter Microplate. *Journal of Geophysical Research*, **96**, 7961–7993.

Nei M (1978) Estimation of average heterozygosity and genetic distance from a small number of individuals. *Genetics*, **89**, 583–590.

Neigel JE (1997) A comparison of alternative strategies for estimating gene flow from genetic markers. *Annual Review of Ecology and Systematics*, **28**, 105–128.

Nielsen R, Wakeley J (2001) Distinguishing migration from isolation: a Markov chain Monte Carlo approach. *Genetics*, **158**, 885–896.

O'Mullan GD, Maas PAY, Lutz RA, Vrijenhoek RC (2001) A hybrid zone between hydrothermal vent mussels (Bivalvia: Mytilidae) from the Mid-Atlantic Ridge. *Molecular Ecology*, **10**, 2819–2831.

Pradillon F, Shillito B, Young C, Gaill F (2001) Developmental arrest in vent worm embryos. *Nature*, **413**, 698–699.

Raymond M, Rousset F (1995a) An exact test for population differentiation. *Evolution*, **49**, 1280–1283.

Raymond M, Rousset F (1995b) GENEPOP Version 1.2: population genetics software for exact tests and ecumenicism. *Journal of Heredity*, **86**, 248–249.

Reid JL (1986) On the total geostrophic circulation of the South Pacific Ocean: flow patterns, tracers and transports. *Progress in Oceanography*, **16**, 1–61.

Rice WR (1989) Analyzing tables of statistical tests. *Evolution*, **43**, 223–225.

Rousset F, Raymond M (1995) Testing heterozygote excess and deficiency. *Genetics*, **140**, 1413–1419.

Sambrook J, Fritsch EF, Maniatis T (1989) *Molecular Cloning, A Laboratory Manual*, 2nd edn. Cold Spring Harbor Press, Cold Spring Harbor, NY.

Schneider S, Roessli D, Excoffier L (2000) *ARLEQUIN, a Software Package for Population Genetics Data Analysis*, Version 2.000. Genetics and Biometry Laboratory, University of Geneva, Geneva, Switzerland.

Searle RC, Rusby RI, Engeln J *et al.* (1989) Comprehensive sonar imaging of the Easter microplate. *Nature*, **341**, 701–705.

Shank TM, Fornari DJ, Von Damm KL *et al.* (1998) Temporal and spatial patterns of biological community development at nascent deep-sea hydrothermal vents (9°50′ N East Pacific Rise). *Deep Sea Research*, **II** (45), 465–515.

Sinton JM, Norby L, Batiza R (1994) Young volcanism at superfast spreading: EPR 17°–19° S. *EOS Transactions American Geophysical Union*, **75**, 320.

Skibinski DOF, Gallagher C, Benyon CM (1994) Mitochondrial DNA inheritance. *Nature*, **368**, 817–818.

Slatkin M (1993) Isolation by distance in equilibrium and non-equilibrium populations. *Evolution*, **47**, 264–279.

Speiss R, MadcDonald K, Atwater T *et al.* (1980) East Pacific Rise: hot springs and geophysical experiments. *Science*, **207**, 1421–1433.

Tunnicliffe V, McArthur AG, Mchugh D (1998) A biogeographical perspective of the deep-sea hydrothermal vent fauna. *Advances in Marine Biology*, **34**, 353–442.

Van Dover CL (2000) *The Ecology of Deep-Sea Hydrothermal Vents*. Princeton University Press, Princeton, NJ.

Van Dover CL, Fry B (1994) Microorganisms as food resources at deep-sea hydrothermal vents. *Limnology and Oceanography*, **39**, 51–57.

Van Dover CL, German CR, Speer KG, Parson LM, Vrijenhoek RC (2002) Evolution and biogeography of deep-sea vent and seep invertebrates. *Science*, **295**, 1253–1257.

Van Dover CL, Hessler RR (1990) Spatial variation in faunal composition of hydrothermal vent communities on the East Pacific Rise and Galapagos spreading center. In: *Gorda Ridge: A Seafloor Spreading Center in the United States' Exclusive Economic Zone* (ed. McMurray GR), pp. 253–264. Springer, New York.

Vinogradova N (1979) The geographical distribution of the abyssal and hadal (ultra-abyssal) fauna in relation to vertical zonation of the ocean. *Sarsia*, **64**, 41–50.

Weir BS, Cockerham CC (1984) Estimating *F*-statistics for the analysis of population structure. *Evolution*, **38**, 1358–1370.

Zal F, Jollivet D, Chevaldonné P, Desbruyères D (1995) Reproductive biology and population structure of the deep-sea hydrothermal vent worm *Paralvinella grasslei* (Polychaeta: Alvinellidae) at 13° N on the East Pacific Rise. *Marine Biology*, **122**, 637–648.

Zouros E, Ball AO, Saavedra C, Freeman KR (1994) An unusual mitochondrial DNA inheritance in the blue mussel *Mytilus*. *Proceedings of the National Academy of Sciences of the USA*, **91**, 7463–7467.

This study is part of Yong-Jin Won's PhD research project with the Ecology and Evolution Program at Rutgers, the State University of New Jersey. His research interests focus on the population genetics of marine organisms. Aspects of statistical population genetics are the main interest of C. Robert Young, PhD student in Department of Ecology and Evolutionary Biology at University of California, Santa Cruz. Robert Vrijenhoek (Professor Emeritus of Genetics at Rutgers University and Senior Scientist at MBARI) focuses his studies on the molecular ecology of marine and aquatic organisms. Richard Lutz (Professor of Marine and Coastal Sciences at Rutgers) is interested in the ecology and evolution of hydrothermal vent organisms.
